Developmental Dynamics

# Cyp1B1 expression patterns in the developing chick inner ear

| | |
|---|---|
| Journal: | *Developmental Dynamics* |
| Manuscript ID | Draft |
| Wiley - Manuscript type: | Patterns & Phenotypes |
| Date Submitted by the Author: | n/a |
| Complete List of Authors: | CARDEÑA-NÚÑEZ, SHEILA; University of Extremadura, Cell Biology<br>SÁNCHEZ-GUARDADO, LUIS OSCAR; California Institute of Technology, Division of Biology and Biological Engineering<br>Hidalgo-Sánchez, Matías; University of Extremadura, Biología Celular |
| Keywords: | Cytochrome P450, Retinoic acid, RALDH, Fgf10, Otic specification, Otic patterning, Sensory patch |
| | |

# *Cyp1B1* expression patterns in the developing chick inner ear

**Sheila Cardeña-Núñez *[1], Luis Óscar Sánchez-Guardado *[2], and Matías Hidalgo-Sánchez [1+]**

[1] Department of Cell Biology, School of Science, University of Extremadura, Badajoz E06071, Spain.

[2] Division of Biology and Biological Engineering, California Institute of Technology, Pasadena, CA, USA.



Running head: *Cyp1B1* in the developing chick inner ear

* These authors contributed equally to this work

[+]Correspondence to: Matías Hidalgo-Sánchez. Department of Cell Biology, University of Extremadura, Avda. de Elvas s/n, 06071 Badajoz, Spain. Tel. and Fax: +34 924289411. E-mail address: mhidalgo@unex.es

**Key words:** Cytochrome P450; retinoic acid; RALDH; Fgf10; otic specification; sensory patch; otic patterning.

**Grant sponsor:** This work was supported by the Spanish Ministry of Science (BFU2010-19461 to M.H.-S.); Junta de Extremadura (GR10152, GR15158, and GR18114 to M.H.-S.). Junta de Extremadura, Fondo Europeo de Desarrollo Regional, "Una manera de hacer Europa" (IB18046 to M.H.-S.); L.-O.S.-G. received a Junta-de-Extremadura predoctoral studentship (PRE/08031).

**Abbreviations**

| | |
|---|---|
| ac | anterior crista |
| AG | acoustic ganglion |
| asc | anterior semicircular canal |
| AVG | acoustic-vestibular ganglion |
| bp | basilar papilla |
| cc | common crus |
| cd | cochlear duct |
| ed | endolymphatic duct |
| es | endolymphatic sac |
| HB | hindbrain |
| hp | horizontal pouch |
| lc | lateral crista |
| lsc | lateral semicircular canal |
| ml | macula lagena |
| mn | macula neglecta |
| ms | macula sacculi |
| mu | macula utriculi |
| pc | posterior crista |
| psc | posterior semicircular canal |
| rh | rhombomere |
| s | saccule |
| tv | tegmentum vasculosum |
| u | utricle |
| vp | vertical pouch |

## Abstract

Retinoic acid (RA) plays an important role in organogenesis as a paracrine signal through transcriptional regulation of an increasing number of known downstream target genes, regulating cell proliferation and differentiation, as well as morphogenesis. During the development of the inner ear, a complex three-dimensional sensorial structure with auditory and vestibular functions, RA directly governs the morphogenesis and specification processes mainly by means of RA-synthesizing retinaldehyde dehydrogenase (RALDH) enzymes. Interestingly, CYP1B1, a cytochrome P450 enzyme, is able to mediate the oxidative metabolisms also leading to RA generation, its expression patterns being associated with many known sites of RA activity. This study describes for the first time the presence of CYP1B1 in the developing chick inner ear as a RALDH-independent RA-signaling mechanism. In our *in situ* hybridization analysis, *Cyp1B1* expression was first observed in a domain located in the ventromedial wall of the otic anlagen, being included within the rostralmost aspect of an *Fgf10*-positive pan-sensory domain. As development proceeds, all identified *Fgf10*-positive areas were *Cyp1B1* stained, with all sensory patches being *Cyp1B1* positive at stage HH34, except the macula neglecta. *Cyp1B1* expression suggested a possible contribution of CYP1B1 action in the specification of the lateral-to-medial and dorsal-to-ventral axes of the developing chick inner ear.

## INTRODUCTION

The vertebrate inner ear is one of the most complex models of organogenesis and cell specification, regulated by intricate molecular systems devoted to the creation of lineage compartments. During early embryogenesis, the inner ear is induced in the embryonic cephalic ectoderm on both sides of the developing hindbrain as the otic placode, which then proceeds to form the otic vesicle, a simple cavity within the head, which subsequently differentiates into the complex three-dimensional sensory structure. This ovoid rudiment undergoes important morphogenetic changes and cell specification to determine sensory and non-sensory areas in the developing membranous labyrinth, as well as otic neurogenesis, all of them involving a great number of molecular interactions (Fekete and Wu, 2002; Bok et al., 2007; Schneider-Maunoury and Pujades, 2007; Alsina et al., 2009; Groves and Fekete, 2012; Wu and Kelly, 2012; Chen and Streit, 2013; Lassiter et al., 2014; Sánchez-Guardado et al., 2014; Nakajima, 2015; Whitfield, 2015; Raft and Groves, 2015; Basch et al., 2016; Fritzsch and Eliott, 2017; Varela-Nieto et al., 2019; among others). During development, diffusible morphogenes, such as FGF, WNT, BMP, SHH, and retinoic acid (RA), take part in establishing gradients from confined sources, in some cases with restricted sinks. These signaling molecules act in a concentration-dependent manner controlling the expression target position-dependent genes (Meinhardt, 2008; Schilling et al., 2012; Durston, 2015; Tuazon and Mullins, 2015; Nesterenko et al., 2017; Dubey et al., 2018). These spatial and temporal dynamics interactions also govern the morphogenetic and specification events occurring during the development of vertebrate inner ears (Romand et al., 2006a; Bok et al., 2007; Ohyama et al., 2007; Schimmang, 2007; Whitfield and Hammond, 2007; Schneider-Maunoury and Pujades, 2007; Chatterjee et al. 2010; Ladher et al., 2010; Wu and Kelley, 2012; Chen and Streit 2013; Munnamalai and Fekete, 2013; Nakajima, 2015; Raft and Groves, 2015; Su et al., 2015; Alsina and Whitfield, 2017; Ebeid and Huh, 2017; Ohta and Schoenwolf, 2018; among others).

RA, a small lipophilic signaling molecule, is the main biologically active metabolite of vitamin A (retinol), playing pleiotropic functions during embryonic development (McCaffery and Dräger, 2000; Tzimas and Nau, 2001; Balmer and Blomhoff, 2002; Blentic et al., 2003; Maden, 2006; Niederreither and Dolle, 2006; Romand et al., 2006a; Hans and Westerfield, 2007; Gudas and Wagner, 2011; Tonk et al., 2015; Xavier-Nieto

et al., 2015; Ealy et al., 2016; Stefanovic and Zaffran, 2017; Piersma et al., 2017; Dubey et al., 2018; Frank and Sela-Donenfeld, 2019). RA biosynthesis occurs in a two-step process: firstly, precursor retinol (vitamin A) is oxidized to retinaldehyde by the cytosolic alcohol dehydrogenases (ADHs) and the retinol dehydrogenases (RDHs); then, retinaldehyde is transformed to RA by members of the aldehyde dehydrogenease (ALDH) class known as retinaldehyde dehydrogenases (RALDH) (Ross et al., 2000; Duester et al., 2003; Blomhoff and Blomhoff, 2006; Dubey et al., 2018). The controlling actions of RA occur by regulation of the activity of the RA nuclear receptor family, the retinoic acid receptors (RARs) and the retinoid X receptors (RXRs), to govern the expression of target genes binding to retinoic acid-response elements (RAREs) present in the regulatory sequences of these RA-regulated genes (Blomhoff and Blomhoff, 2006; Mark et al., 2006; Gudas and Wagner, 2011; Benbrook et al., 2014). In addition, RA is degraded by oxidative inactivation by members of the cytochrome P450 family, the so-named CYP26A-C1 enzymes (Thatcher and Isoherranen, 2009; White and Schilling, 2008; Pennimpede et al., 2010). The appropriate distribution of RA within embryonic tissues is determined, therefore, by the balance between its synthesis and its degradation, this being essential for normal development (reviewed in Ross et al., 2000; Romand et al., 2006a; Pennimpede et al., 2010; Piersma et al., 2017).

Cytochrome P450 (CYP) enzymes are a widespread superfamily of ubiquitously distributed enzymes with a heme-binding domain involved in the oxidation of a varied range of endogenous and xenobiotic substrates (Nelson, 2011, 2018; see also Baldwin et al., 2009; Zhanger and Schwab, 2013; Dejong and Wilson, 2014). The *CYP1* gene family consists of three closely related genes classified into two subfamilies (*CYP1A1*, *CYP1A2*, *CYP1B1*; Godard et al., 2000, 2005; Zanger and Schwab, 2013) and one pseudogene *CYP1D* (Godard et al., 2000, 2005; see also El-kady et al., 2004a,b; Itakura et al., 2005; Jönsson et al., 2007). In particular, CYP1B1 was first identified in mouse embryo fibroblast-derived cell line and rat adrenal gland cells (Pottenger et al., 1991; Otto et al., 1991, 1992), encoded by mouse, rat, and human CYP1B1 orthologous genes (Bhattacharyya et al., 1995; Savas et al., 1994; Sutter et al., 1994; Tang et al., 1996; Murray et al., 2001). As a dioxin-inducible enzyme, CYP1B1 is clinically relevant in cancer induction, neoplastic progression, and malignant tumour metabolism of a wide range of human cancers (Murray et al., 2001; Sissung et al., 2006). In particular, *Cyp1B1* mutations are the most frequent cause of primary congenital glaucoma (Chavarria-Soley

et al., 2008; Vasiliou and Gonzalez, 2008; Badeeb et al., 2014). Apart from these studies of glaucoma, the histopathological and physiological characterizations of *Cyp1B1*-null mice showed no alterations with respect thtoe wild mice, suggesting a redundant and compensatory action with other related genes (Buters et al., 1999).

Unlike CYP26A-C1 enzymes, CYP1B1 is unable to further metabolize RA to any of its less active products. CYP1B1 is involved in RA synthesis during patterning events in chick embryos, catalysing the conversion of retinol to retinaldehyde through a RALDH-independent pathway (Chen et al., 2000; Zhang et al., 2000; Choudhary et al., 2004; Chambers et al., 2007). Therefore, CYP1B1 could be an excellent candidate to regulate RA-mediated developmental processes as an additional source of RA. Using several methodological approaches, constitutive CYP1B1 expressions were found in a great number of both embryonic and adult tissues, such as visual and central nervous systems, branchial arches, heart, kidney, limbs, among others (Otto et al., 1992; Sutter et al., 1994; Savas et al., 1994; Bhattacharyya et al., 1995; Christou et al., 1995; Shimada et al., 1996; Murray et al., 1997; Hakkola et al., 1997; Vadlamuri et al., 1998; Rieder et al., 2000; Muskhelishvili et al., 2001; Bejjani et al., 2002; Choudhary et al., 2003, 2005; Stoilov et al., 2004; Xu et al., 2004; Doshi et al., 2006; Chambers et al., 2007; Jönsson et al., 2007; Yin et al., 2008; Palenski et al., 2013; Williams et al., 2015, 2017). The regulation, metabolic specificity, and tissue-specific expression has been reviewed, with it playing a key role in several physiological aspects in vertebrates (Murray et al., 2001; see refs. therein).

In addition to the already reported expression patterns of *Raldh* genes, detailed studies about the expression of *Cyp1B1* may help to understand the role of the RA signaling pathway in the morphogenesis and sensory specification occurring during the development of the vertebrate inner ears. In this sense, we have performed a comprehensive analysis of the mRNA expression of *Cyp1B1* through several developmental stages of the chick inner ear (from stage HH18-20 to HH34). We found that *Cyp1B1* expression was first observed in a domain located in the ventromedial wall of the otic anlagen, being included within the *Fgf10*-positive pan-sensory domain (Sánchez-Guardado et al., 2013), but excluding the presumptive territory of the *Fgf10*-positive posterior crista. Shortly after, the *Cyp1B1*-expression extended caudally to then include the aforementioned territory. At stage HH24, all identified *Fgf10*-positive areas

were *Cyp1B1* stained, with the levels of *Cyp1B1* expression being higher in the anterior and posterior cristae and lower in the utricular and saccular maculae, as well as in the basilar papilla. At stage HH27, the lateral crista was clearly *Cyp1B1* positive. At stage HH34, when all sensory patches are clearly identified (Sánchez-Guardado et al., 2013), all these patches were *Cyp1B1* positive except the macula neglecta. Interestingly, several areas of the mesenchyme underlying the otic epithelium showed a strong CYP1B1 expression, clearly suggesting the involvement of CYP1B1 activity in the establishment of the lateral-to-medial and dorsal-to-ventral axes of the developing chick inner ear. New studies would be required to evaluate the involvement of CYP1B1 in the development of this sensory organ.

## Material and Methods

### Tissue processing

Chick embryos were obtained from fertilized White Leghorn chick eggs incubated in a humidified atmosphere at 38°C. All embryos were treated according to the recommendations for laboratory animals of the European Union and of the Spanish government. Embryos ranging between stages HH18 and HH34 (Hamburger and Hamilton 1951) were fixed by immersion in 4% paraformaldehyde in 0.1M phosphate-buffered saline solution (PBS, pH 7.4) at 4°C overnight. The fixed embryos were rinsed and cryoprotected in 10% sucrose solution in PBS, and were then embedded in the same buffered sucrose solution with added 10% gelatin. The blocks were frozen for 1 min in isopentane cooled to -70°C by dry ice, and then stored at -80°C. Cryostat serial sections 20 μm thick were cut in the transverse and horizontal planes, mounted as parallel sets on SuperFrost slides, and stored at -80°C until use. Twenty embryos were used per stage.

### *In situ* hybridization staining procedure

*In situ* hybridization was performed on cryosections as described by Sánchez-Guardado et al. (2009, 2011, 2013). The *Cyp1B1* probe was obtained with Not1 and T3 enzymes to generate antisense probes. The *Fgf10* probes were the same as used previously (Sánchez-Guardado et al. 2013). All riboprobes were labeled with digoxigenin-11-UTP (Roche, Mannheim, Germany) according to the manufacturer's instructions. *In situ* hybridization was performed on cryosections following the methods described by Sánchez-Guardado

et al. (2009, 2013). The sections were post-fixed with 4% paraformaldehyde in PBS for 10 min, then rinsed with PBS for 15 min. The sections were acetylated in a solution containing 234 ml of $H_2O$-d, 3.2 ml of triethanolamine (Sigma), 420 ml of 36% HCl, and 600 ml of acetic anhydride. After acetylation, the sections were permeabilized in 1% Triton X-100 for 30 min, and then pre-hybridized at room temperature for 2 h in a solution containing 50% formamide, 10% dextran sulfate (Sigma), 5x Denhardt's solution (Sigma), and 250 mg/ml t-RNA (Roche), in salt solution. Hybridization was performed with 200-300 ng/ml of the probe in the same hybridization solution overnight at 72°C. After hybridization, the sections were rinsed with 0.2% SSC at 72°C for 1-2 h, and then twice with a solution containing 100 mM NaCl and 100 mM Tris-HCl (pH 7.5). After treatment with 10% normal goat serum (NGS) in the same solution for 2 h, the sections were incubated overnight with alkaline phosphatase-conjugated anti-digoxigenin Fab fragments (Roche, 1:3500). The sections were rinsed twice with the same buffer, and then incubated in 100 mM NaCl, 50 mM $MgCl_2$, and 100 mM Tris–HCl (pH 9.5). The colouring reaction was developed with NBT and BCIP (Roche). The sections were rinsed with PBS and coverslipped with Mowiol (Calbiochem, Bad Soden, Germany). No signal was obtained with the sense probes. For more details about the in situ hybridization procedure, see Ferran et al. (2015).

**Immunohistochemistry staining procedure**

Immunohistochemistry with 3A10 antibody (1:40; Antibody ID from NIF: AB_531874; Developmental Studies Hybridoma Bank (DSHB), mouse, monoclonal, #3A10; Sánchez-Guardado et al. 2013) was also performed on cryosections as previously described by Sánchez-Guardado et al. (2009, 2011, 2013). The primary antibody was reacted with biotinylated goat anti-mouse secondary antibody (1:100; Sigma), and then with ExtrAvidin-biotin-horseradish peroxidase complex (1:200; Sigma). All antibodies were diluted in a solution containing 1% NGS and 0.25% Triton X-100 in PBS. The histochemical detection of the peroxidase activity was carried out by using 0.03% diaminobenzidine (DAB) and 0.005% $H_2O_2$. After the immunoreactions, the sections were rinsed three times with PBS-T and then coverslipped with Mowiol.

**Imaging**

All preparations were photographed with a Zeiss Axiophot microscope equipped with a Zeiss AxioCam camera (Carl Zeiss, Oberkochen, Germany) and AxioVision 2.0.5.3.

software, and the images were saved in 4-MB TIFF format. These were size-adjusted, cropped, contrast-enhanced, and annotated with Adobe Photoshop version 7.0 software (Adobe Systems, San Jose, CA). All illustrations were produced with this Adobe Photoshop software.

## Results

### *Cyp1B1* expression pattern at the otic vesicle stage (HH18-20)

In transverse sections through the otic vesicle stage (ov; HH18-20), *Cyp1B1* transcripts were detected in its ventromedial wall (white arrow in Fig. 1A), included within the *Fgf10*-expressing pan-sensory domain (white arrow in Fig. 1B; Sánchez-Guardado et al. 2013). To better analyse the relationship between the *Cyp1B1*- and *Fgf10*-positive areas, horizontal sections were also studied (Fig. 1C, D). Weak *Cyp1B1* expression was observed all along the medial wall of the otic vesicle (white arrow in Fig. 1C), except in its caudalmost portion (black arrow in Fig. 1C). In the most rostral aspect of the otic vesicle, the *Cyp1B1*-positive domain included the presumptive territory of the *Fgf10*-labeled anterior crista (ac in Fig. 1C, D; see also Sánchez-Guardado et al., 2013), whereas in its most caudal portion, the caudal *Cyp1B1*-negative domain contained the *Fgf10*-labeled posterior crista (pc in Fig. 1C, D). At this developmental stage, the acoustic-vestibular ganglion displayed very weak, almost undetectable, *Cyp1B1* expression (AVG; black asterisk in Fig. 1C). Interestingly, the mesenchyme located between the otic epithelium and the hindbrain appeared strongly *Cyp1B1* labeled (white asterisk; Fig. 1A, C), being *Cyp1B1* negative that located between the otic vesicle and the cephalic ectoderm (blue asterisk in Fig. 1C). Figure 1E and 1F summarize the *Cyp1B1* expression pattern in the wall of the otic vesicle.

### *Cyp1B1* expression pattern at stages HH24/25

At stage HH24, the inner ear shows significant morphogenetic changes and the presumptive territories of almost all sensory patches are clearly identified on cryostat sections treated with *Fgf10* probes (Fig. 2; Sánchez-Guardado et al. 2013). In dorsal horizontal sections (Fig. 2A, B), *Cyp1B1* expression appeared in the anterior portion of the otic anlage (Fig. 2A), coinciding with the *Fgf10*-positive anterior crista (ac; between arrowheads in Fig. 2B). Another small area of *Cyp1B1* expression was also observed in

the caudalmost wall of the stage HH24/25 inner ear, being coincident with the *Fgf10*-positive posterior crista (pc; Fig. 2B), and exhibiting also several small domains of *Cyp1B1* expression. Therefore, the posterior crista was *Cyp1B1* positive at stage HH27 but not at stage HH20 (compare Fig. 2A, B with Fig. 1C, D). In more ventral horizontal sections (Fig. 2C, D), the *Fgf10*-stained macula utriculi displayed a weak *Cyp1B1* expression (mu in Fig. 2C, C'). The developing lateral crista, which develops just lateral to the macula utriculi and shows an incipient *Fgf10* expression at this developmental stage (lc in Fig. 2D; Sánchez-Guardado et al., 2013), showed Cyp1B1 transcripts in a very narrow band just in its medial portion, abutting the presumptive macula utriculi (lc in Fig. 2C). At this level, the macula sacculi was *Cyp1B1* labeled (Fig. 2C'), but not the macula neglecta (mn in Fig. 2D). Horizontal sections through the developing cochlear duct (cd; Fig. 2E, F) showed a clear *Cyp1B1* expression in the basilar papilla (bp; between arrowheads in Fig. 2E, F). The rest of the cochlear wall was devoid of *Cyp1B1* expression (Fig. 2E). Outside of the otic epithelium, *Cyp1B1* transcripts were seen in the mesenchyme between the otic epithelium and the hindbrain (HB; white asterisks in Fig. 2A, C) at the level of the vestibular apparatus. Regarding the auditory system, the mesenchyme rostral to the developing cochlear duct showed a strong *Cyp1B1* expression (cd; rostral white asterisk in E). Nevertheless, other areas of the mesenchyme near the wall of the cochlear duct showed a weak *Cyp1B1* expression (caudal white asterisk in Fig. 2E). It is interesting to remark that areas of the periotic mesenchyme were completely devoid of *Cyp1B1* transcripts, in particular in the lateral aspect of the otic anlagen (purple asterisks in Fig. 2A, C, E).

Transverse sections through an inner ear at the more developed stage HH25 showed a clearer differentiation of sensory patches (Fig. 2G-L). These sections confirmed previously described results in horizontal sections concerning the presence of *Cyp1B1* expression in the *Fgf10*-positive anterior and posterior cristae (ac and pc; between arrowheads in Fig. 2G, H and Fig. 2K, L, respectively). At the vestibular level, it could now be appreciated that *Cyp1B1* labeling was strong in lateral crista (lc; Fig. 3I) and weaker in macula utriculi (mu; Fig. 2I) and macula sacculi (ms in Fig. 2I). Furthermore, *Cyp1B1* transcripts could be observed in the basilar papilla (bp; Fig. 2I, J). In the most caudal sections (Fig. 2K, L), the *Fgf10*-negative macula neglecta was *Cyp1B1* negative (mn in Fig. 2K, L). Outside the otic epithelium, the mesenchyme surrounding the ventral half of the the stage HH24/25 inner ear was clearly labeled by different intensities of

*Cyp1B1* expression, mainly in the medial and ventrolateral aspects of the stage HH25 inner ear (white asterisks in Fig. 2G, I, K). Other areas of the periotic mesenchyme did not express this gene (purple asterisks in Fig. 2G, I, K). The acoustic-vestibular ganglion was almost completely devoid of *Cyp1B1* expression, except in a small part of its ventral aspect (short arrow in Fig. 2G). Figure 3M and 3N summarize the *Cyp1B1* expression pattern in the otic epithelium at stages HH24/25.

### *Cyp1B1* expression patterns at stage HH27

At stage HH27, the morphogenetic changes are more evident and all the sensory epithelia are easily recognized by the *Fgf10* expression pattern (Fig. 3; Sánchez-Guardado et al., 2013). In horizontal sections through the dorsalmost portion of the stage HH27 inner ear (Fig. 3A, B), *Cyp1B1* expression appeared in the *Fgf10*-positive anterior and posterior cristae (ac and pc; between arrowheads in Fig. 3A, B). In more ventral horizontal sections across the central aspect of the vestibule (Fig. 3C, D), all the *Fgf10*-positive sensory patches displayed different grades of *Cyp1B1* expression: a strong *Cyp1B1* stain in the lateral crista (lc; between arrowheads in Fig. 3C, C', D) and a weak *Cyp1B1* labelling in central part of both the macula utriculi and the macula saculi (mu and ms in Fig. 3C, D). The macula neglecta was devoid of *Cyp1B1* expression (not shown). *Cyp1B1* transcripts were absent in the epithelium of all non-sensory elements, for example the horizontal and vertical pouches (hp and vp in Fig. 3A) and the endolymphatic apparatus (ed in Fig. 3A). In addition, the acoustic-vestibular ganglion was apparently devoid of *Cyp1B1* transcripts (AVG in Fig. 3C). At the most ventral level of the stage HH27 inner ear (Fig. 3E, F), where the auditory system develops, the *Fgf10*-positive basilar papilla was *Cyp1B1* stained (bp; between arrowheads in Fig. 3E, F). The *Cyp1B1* expression observed in the basilar papilla extended more rostrally than the *Fgf10*-expressing domain (arrow in Fig. 3E, F; Sánchez-Guardado et al., 2013). At the end of the cochlear duct (cd; Fig. 3G, H), the incipient specified *Fgf10*-positive macula lagena also showed an evident, although weaker, *Cyp1B1* expression (ml in Fig. 3G, H). The differentiating acoustic ganglion was without *Cyp1B1* transcripts (AG in Fig. 3E). Outside of the developing membranous labyrinth, the mesenchyme located between the developing inner ear and the hindbrain (HB; Fig. 3A) was strongly labeled by the *Cyp1B1* expression in the dorsal aspect of the inner ear (white asterisks in Fig. 3A, C, C'). It is also interesting to remark that the acoustic-vestibular ganglion was completely surrounded by mesenchyme expressing

strongly the *Cyp1B1* gene, as well as the utricular and saccular maculae (see the rostralmost white asterisks in Fig. 3C, C'). At this level, the mesenchyme next to the caudal otic wall also showed a very evident *Cyp1B1* expression (caudalmost asterisks in Fig. 3C). At the level of the vestibular apparatus, the mesenchyme between the otic anlagen and the cephalic ectoderm was completely devoid of *Cyp1B1* expression (purple asterisks in Fig. 3A, C), including the areas surrounding the developing cristae (ac and pc in Fig. 3A; lc in Fig. 3C). In the ventral half of the inner ear, where the auditory system develops (Fig. 3E, F), the *Cyp1B1* labeling appeared also surrounding the otic epithelium, mainly at the lateral portions (white asterisks in Fig. 3E). Transverse sections confirmed the results described before (data not shown). Figure 3I and 3J summarize the *Cyp1B1* expression pattern in the otic epithelium at stages HH27.

### *Cyp1B1* expression patterns at stage HH34

At 8 days of incubation (stage HH34), all the sensory and non-sensory elements of the inner ear are clearly defined (Sánchez-Guardado et al. 2013). At this developmental stage (Fig. 4), the horizontal sections show no changes of the *Cyp1B1* expression pattern compared with the results described at stage HH27 (Fig. 3). In a dorsal horizontal section, *Cyp1B1* staining appeared in the anterior and posterior cristae (ac and pc; between arrowheads in Fig. 4A). The macula neglecta, located next to the posterior crista, was *Cyp1B1* negative (mn in Fig. 4A). The rest of the otic epithelium was completely without *Cyp1B1* labeling, including the wall of the endolymphatic apparatus (ed in Fig. 4A; es, not shown) and the common crus (cc in Fig. 4A). As in previous developmental stages, the mesenchyme just underlying the membranous labyrinth showed a very evident *Cyp1B1* expression (white asterisks in Fig. 4A). At the level of the utricule and saccule (u and s; Fig. 4B), all the sensory patches displayed *Cyp1B1* labeling in different grades: the lateral crista (lc; between arrowheads in Fig. 4B); the macula utriculi, with a strong *Cyp1B1* expression (mu in Fig. 4B); and the macula saculi, with a weaker *Cyp1B1* expression (ms; Fig. 4B). In this section, the medial wall of the proximal cochlear duct, near the macula sacculi, was also *Cyp1B1* positive (arrow in Fig. 4B). The vestibular ganglion was *Cyp1B1* negative (VG in Fig. 4B'). A striking result was the strong expression of *Cyp1B1* in the mesenchyme in contact with and even from a distance of the otic epithelium (asterisks in Fig. 4B, B'). Horizontal sections through the intermediate cochlear duct, the basilar papilla displayed a rostral-to-caudal decreasing gradient of *Cyp1B1* expression (bp; between arrowheads in Fig. 4C). The macula lagena displayed

low levels of *Cyp1B1* transcripts (ml in Fig. 4D). The non-sensory areas of the cochlear duct, including the tegmentum vasculosum (tv in Fig. 4C), were *Cyp1B1* negative Fig. 4C, D). With respect to the acoustic ganglion, this neuronal structure was also devoid of *Cyp1B1* expression (AG in Fig. 4C). The *Cyp1B1*-lebeled mesenchyme appeared surrounding practically the whole wall of the cochlear duct (Fig. 4C, D), with this *Cyp1B1*-expressing mesenchyme being less relevant in its aspect of the cochlear duct. Figure 4E and 4F summarize the *Cyp1B1* expression pattern in the membranous labyrinth at stage HH34.

## Discussion

The Retinoic acid (RA) directly controls the morphogenesis and specification mechanisms during the development of vertebrate inner ears, mainly by means of RA-synthesizing RALDH enzymes (reviewed by Romand et al., 2006a; Frenz et al., 2010; Wu and Kelly, 2012; Nakajima, 2015; Raft et al., 2015; see also Romand et al., 2013). In the developing mouse inner ear, *Raldh1-3* genes have restricted and dynamic expression patterns with overlapping domains (Niederreither et al., 2002; Romand et al., 2001, 2004, 2006a, b). In other vertebrate, the *Raldh3* expression patterns display manifest similarities at the developmental stages analysed (*Xenopus*: Lupo et al., 2005; zebrafish: Pittlik et al., 2008; chick: Mic et al., 2000; Sánchez-Guardado et al., 2009). The detailed expression pattern reported in chick embryos showed that RA is produced in the dorsomedial portion of the otic vesicle (Sánchez-Guardado et al., 2009). At the earlier developmental stages, this morphogene might diffuse towards ventral areas controlling the whole patterning of the otic rudiment as a long-range signal acting through dose-dependent effects (Sánchez-Guardado et al., 2009). Therefore, these RA-synthesizing RALDH enzymes could be directly involved in determining morphogenetic events and sensory patch specification during the development of this complex sensorial organ.

Chambers and co-workers have shown that, *in vitro*, CYP1B1 itself produces both all-trans-retinal (t-RAL) and all-trans-retinoic acid (t-RA), thus contributing to the synthesis of RA involved in the patterning of several embryonic tissues (Chambers et al., 2007; see also Zhang et al., 2000; Choudhary et al., 2004). Unlike the CYP26 enzymes, CYP1B1 cannot participate in the degradation of t-RA. Interestingly, the expression patterns of the

chick *Cyp1B1* orthologue during early development is associated with many known sites of RA activity (Chambers et al., 2007). Chick CYP1B1 enzyme participates in the specification of the dorsoventral axis of the neural tube and the acquisition of a motor neuron fate, as well as in the patterning of the epibranchial placodes and the neurogenetic events occurring in them. Furthermore, CYP1B1 activity is exclusively responsible for RA synthesis in the hindbrain paraxial mesoderm, the branchial arches, and the posterior limb bud where *Raldh* expressions are absent (Chambers et al., 2007). In zebrafish, it has been shown that *Cyp1B1* also shows a clear spatial and temporal expression pattern in the eye, diencephalon and midbrain-hindbrain domain, branchial arches, limb, and kidney (Yin et al., 2008). Therefore, chick CYP1B1 constitutes an evident RALDH-independent pathway of RA signaling regulation contributing to the patterning and specification of several developing systems (Chambers et al., 2007; Yin et al., 2008; see also Introduction), including the inner ear (this work).

***Cyp1B1* expression at otic vesicle stage: Patterning and Morphogenesis**

Regarding the developing inner ear, sensory organ specification may be governed by short-range signals from the otic epithelia itself or from the surrounding tissues. In chick embryos of stage HH12+, *Cyp1B1* expression is evident in the ectoderm immediately anterior to the otic vesicle (Chambers et al., 2007). A detailed description of the *Cyp1B1* expression pattern would be essential to understand the role of the retinoic signaling pathway in the morphogenesis of this sensory organ, and in the specification of sensory and non-sensory areas as an additional source of RA (this work). In the otic vesicle epithelium (stage HH20), *Cyp1B1* expression was observed in an anterior-to-posterior band located in the ventromedial portion of the otocyst wall. This *Cyp1B1* expressing domain was coincident in part with the pro-sensory *Fgf10*-expressing domain (Sánchez-Guardado et al., 2013). The presumptive territory of the future posterior crista, located in the caudalmost aspect of the otic anlagen, was the only sensory area that was *Fgf10*-positive and *Cyp1B1*-negative. It seems possible that, in this developmental period, the RA-generating CYP1B1 activity could be involved in the specification of the pro-sensory domain along the anterior-to-posterior axis of the otic anlagen. On the other hand, the RALDH3 activity is, as yet, the main known source of RA in the developing chick inner ear (Sánchez-Guardado et al., 2009). As mentioned above, *Raldh3* expression is observed in the dorsomedial portion of the otic vesicle, in an area corresponding to the presumptive domain of the endolymphatic apparatus, and at a distance from the *Fgf10*-positive pro-

sensory domain at stage HH20 and bordering it at stage HH24 (see Sánchez-Guardado et al., 2013). Therefore, RA generated by RALDH3 and CYP1B1 enzymes within the otic epithelium itself could participate to some extent in the specification of the dorsal-to-ventral and anterior-to-posterior axes of the otic vesicle, respectively.

The generation of RA from nearby tissues should be regarded also as an instructive action towards the developing otic epithelium. It is well accepted that RA generated from the underlying mesenchyme by RALDH activities should participate directly in the specification of the neural tube along its anterior-to-posterior and dorsal-to-ventral axes (Niederreither et al., 2000; Wilson and Maden, 2005; Glover et al., 2006; Maden, 2006; Mark et al., 2006; White and Schilling, 2008; Schilling et al., 2013; Allodi and Hedlund, 2014; Piersma et al., 2017). Similarly, RA from the periotic mesenchyme would control the regionalization of the developing otic epithelium in a stage-dependent manner (Romand et al., 2006a; Pittlik et al., 2008; Braunstein et al., 2009; Bok et al., 2011; Monks and Morrow, 2012; Wu and Kelly, 2012; Maier and Whitfield, 2014; Nakajima et al., 2015; Raft et al., 2015). In the chick, *Raldh2* is expressed in the mesoderm caudal to the otic placode, and an appropriate spatial and temporal concentration of the diffusible RA is necessary for the correct specification of the anterior-posterior axis of the developing otic anlagen (Bok et al., 2011). In this sense, it has been suggested that the CYP1B1-mediated RA synthesis in the paraxial mesoderm could also participate directly in the dorsal-to-ventral specification of the developing neural tube in a paracrine manner (Chambers et al., 2007). Interestingly, the mesenchyme underlying the otic epithelium also expressed the *Cyp1B1* gene in the chick (this work). For more details about the developing vestibular system, chick *Cyp1B1* expression was undoubtedly observed in the mesenchyme between the otic epithelium and the wall of the developing neural tube from stages HH20 to HH27, being completely absent in the mesenchyme between the otic epithelium and the cephalic ectoderm. Therefore, this CYP1B1 activity could determine the specification of the medial versus lateral aspect of the vestibular apparatus. Concerning the auditory system, which develops from the ventral part of the otic anlagen, *Cyp1B1* expression was observed in all the underlying mesenchyme, with greater expression in its anteromedial and posterolateral parts at stages HH24-27 and in its proximal part at stage HH34. Therefore, chick CYP1B1-mediated RA production from the periotic mesenchyme would also contribute to the dorsal-ventral and anterior-posterior specification during inner ear development, instructing the developing

membranous labyrinth, especially due to the absence of RALDH activities in this mesenchyme in avian (Chambers et al., 2007; Sánchez-Guardado et al., 2009). In other vertebrates, a mutual cooperation between CYP1B1 and RALDH1-3 activities has been detected in the periotic mesenchyme (Romand et al., 2006a; Pittlik et al., 2008).

**Specification of the cristae and semicircular canals**

RA contributes to the differentiation of vestibular sensory elements. As mentioned above, *Cyp1B1* expression was present in an anterior-to-posterior oriented band located in the ventromedial part of the otic vesicle, being included in the *Fgf10*-positive pro-sensory domain. At this developmental stage, the presumptive territory of the posterior crista was the only area devoid of *Cyp1B1* expression. As development proceeded, the *Cyp1B1* expressing domain extended caudally, and, at stage HH24/25, the posterior crista was therefore clearly *Cyp1B1* labeled. A particular point has to be mentioned about the lateral crista. At stage HH24, the lateral crista was *Cyp1B1* positive exclusively in a narrow band adjacent to the macula utriculi. Just afterwards, at stage HH25, the lateral crista was clearly labeled by *Cyp1B1* expression, suggesting that the mentioned *Cyp1B1*-stained band observed at stage HH24 had increased in thickness and extended towards the lateral aspect of the lateral crista. Thus, strong *Cyp1B1* expressions were detected in all the cristae from stages HH27 to HH34, suggesting that CYP1B1-mediated RA synthesis could participate in the specification of the cristae. In this sense, it has previously been reported that there is RALDH3 activity in areas adjacent to all the cristae at stage HH24, not overlapping with the *Cyp1B1*-expressing domains. At stage HH27, some *Raldh3*-positive cells were detected within the periphery of all cristae (Sánchez-Guardado et al., 2009), therefore also expressing the *Cyp1B1* gene. The existence of two different sources of RA, probably with different mechanisms of regulation, activation, or inhibition, points to the need for new research in cristae specification.

A clear relationship between the expression patterns of RA-synthesizing *Raldh3* gene and those of other signalling pathways, such as BMP4 and FGF, has been reported previously (Sánchez-Guardado et al., 2009; see also Sánchez-Calderón et al., 2004, 2007). The *Bmp4* gene shows a RARE motif. Therefore, it is considered to be a potential target of the RA regulating pathway (Thompson et al., 2003). The *Bmp4* gene is negatively regulated by RA since RA-soaked beads implanted into the otic vesicle led to an evident reduction of *Bmp4* expression in the developing anterior crista (Choo et al., 1998). Also, RA regulates

FGF3 and FGF10 activities in the developing otic epithelium because changes in RA levels lead to down-regulations of FGF3/FGF10 signaling molecules (Frenz et al., 2010; Cadot et al., 2012; Liu et al., 2008; see Olaya-Sánchez et al., 2016 for chick *Fgf3* and *Fgf10* genes). In addition, several transcription factors could also be involved in the cristae specification. *Meis* genes, belonging to the TALE family, are important targets of RA, cooperating with it in a dose-dependent manner in the proximo-to-distal limb patterning (Roselló-Díez et al., 2014). In the developing chick inner ear, *Meis1* and *Meis2* genes are clearly expressed in the entire presumptive domain of the semicircular canals and more weakly in all associated cristae (Sánchez-Guardado et al., 2011). Besides, RA signaling would control *Irx* expressions (Gómez-Skarmeta et al., 1998). In the developing neural tube, *Irx3* is induced by RA and repressed by FGF (Novitch et al., 2003; Wilson and Maden, 2005), and in embryos deficient in RA signaling, expression of *Irx3* is severely reduced (Diez-del-Corral et al., 2003). In the chick otic vesicle, *Irx* genes are absent or weakly expressed in the presumptive territory of the *Raldh3*-positive endolymphatic apparatus (Sánchez-Guardado et al. 2009), suggesting a repression of *Irx* genes during the development of this non-sensory element. However, RA inhibits *Irx1* and *Irx2* expressions through a BMP-independent mechanism in the developing chick limb (Díaz-Hernández et al., 2013). The possible implication of RA in inducing or repressing *Irx* gene expressions needs further consideration in the developing vertebrate inner ear.

**Specification of maculae**

In the developing chick inner ear, the macula utriculi and macula sacculi displayed weak expressions of the *Cyp1B1* gene at stage HH24. At stages HH27 and HH34, the *Cyp1B1* expression was maintained in the utricular and saccular maculae. An additional *Cyp1B1* expression was detected in the macula lagena, while the macula neglecta being *Cyp1B1* negative. With respect to the RALDH3 activity as a source of RA, the *Raldh3*-expressing domain was observed in the dorsomedial wall of the chick otic anlagen at stage HH24, bordering dorsally the undifferentiated utricular/saccular maculae (Sánchez-Guardado et al., 2013). It was proposed that the RA signaling mechanism may define limits in the developing membranous labyrinth, such as the precise location of the *Raldh3-Gbx2/Bmp4-Fgf8* boundary (Sánchez-Guardado et al., 2013). Results of work in the developing neural tube, showing that RA from the somites blocks the FGF signaling

pathway (Diez-del-Corral et al., 2003; Wilson and Maden, 2005), would support the descriptive findings reported by Sánchez-Guardado and co-workers (Sánchez-Guardado et al., 2013). At stage HH27, chick *Raldh3* expression is present mainly bordering the utricula and saccular maculae, and there are even *Raldh3*-positive cells in some areas of these sensory patches, similar results to those observed in the macula lagena at stage HH34. The chick macula neglecta is always bordered by *Raldh3* expression (Sánchez-Guardado et al., 2013). Chick *Cyp1B1* expression in the maculae was observed in the utricular and saccular maculae, as well as with less intensity in the macula lagena, but not outside these sensory elements. Some parts of them showed an overlapping expression of the two genes. In view of all these results together, a key question would be to know the possible regulating mechanisms of RALHD3 and CYPB1 activities and their interaction with other signaling pathways and transcription factors during the specification of inner ear maculae in vertebrates.

**Specification of the basilar papilla**

RA is directly involved in auditory system development, so that changes of RA levels lead to severe alteration of the cochlea (see Romand et al., 2006a for a review) and hair cell specification in the auditory sensory element (Thiede et al., 2014). In the mouse, *Raldh1* was observed in the Kölliker's organ while *Raldh2* and *Raldh3* was present in the stria vascularis and the Reissber membrane. CYP26 metabolic enzymes and cellular RA binding proteins are also present in the developing cochlear canal and the underlying mesenchyme. In addition, several components of the developing cochlear duct exhibit *RAR* and *RXR* expressions, with *RARα/RARγ* mutant mice showing major perturbations during their development (see Romand et al., 2006a). In the chick inner ear, *Raldh3* expression is also present in the developing cochlear duct (Sánchez-Guardado et al., 2009), and the perturbation of the RA doses by the implantation of RA-soaked beads confirms its direct involvement in the specification of the auditory system (Choo et al., 1998). The *Cyp1B1* positive area included the basilar papilla and the rostralmost portion contiguous to this auditory system (this work). As development proceeded, the basilar papilla exhibited a decreasing rostral-to-caudal gradient of *Cyp1B1* expression (stage HH34). All the non-sensory elements of the auditory apparatus were *Cyp1B1* negative except a small area of the proximal cochlear duct. Therefore, Cyp1B1 activity, not considered until now in the development of the auditory system, could play a key role in

that system's cellular specification, so that new research should be considered in this regard.

In summary, CYP1B1 activity may participate in specification events that confer positional identity in the developing membranous labyrinth, defining the location and extension of sensory patches. More experimental studies are required to determine the role of RA produced by CYP1B1 in inner ear development through the cooperation of CYP26 metabolic enzymes, cellular RA binding proteins, and RAR/RXR, regulating the increasing number of genes known to be directly or indirectly regulated by RA (Balmer and Blomhoff, 2002; Romand et al., 2013; Savory et al., 2014). In this sense, it seems to be possible that CYP1B1 may play an important role in the morphogenesis and specification of the inner ear via the synthesis of alternative, unidentified, regulatory factors, different from RA, as was suggested by Chambers and co-workers. Moreover, other as yet unidentified RA-synthesising enzymes could also be considered (Chambers et al., 2007).

**Acknowledgements**

We thank the members of our scientific group for helpful discussions. This work was supported b:y the Spanish Ministry of Science (BFU2010-19461 to M.H.-S.); Junta de Extremadura (GR10152, GR15158, and GR18114 to M.H.-S.); Junta de Extremadura, Fondo Europeo de Desarrollo Regional, "Una manera de hacer Europa" (IB18046 to M.H.-S.); and L.-O.S.-G. received a Junta-de-Extremadura predoctoral studentship (PRE/08031).

**Conflict Of Interest Statement**

The authors declare no conflict of interest.

Compliance with ethical standards.

## Figure legends

**Fig. 1. *Cyp1B1* expression pattern at the otic vesicle stage, HH18-20**. Transverse (**A**, **B**) and horizontal (**C**, **D**) sections were treated with the *Cyp1B1* and *Fgf10* probes. The *Cyp1B1* and *Fgf10* expressions were observed in the medial wall of the otic vesicle (white arrows in **A-D**), excluding the presumptive domain of the *Fgf10*-stained posterior crista (pc; back arrows in **C**, **D**). The black asterisk in **c** designates a weak *Cyp1B1* expression in the acoustic-vestibular ganglion. The white and purple asterisks in **A** and **C** label the periotic mesenchyme expressing or not the *Cyp1B1* gene, respectively. **E**, **D:** 3D diagrams of *Cyp1B1* expression patterns at the otic vesicle stage, HH18-20, in anterior (**E**) and posterior (**D**) views. Dotted areas show the *Fgf10*-positive sensory domain. For other abbreviations, see the list. Orientation: A, anterior; D, dorsal; M, medial; P, posterior.

**Fig. 2. *Cyp1B1* expression patterns at stage HH24. A-F:** Horizontal sections treated with the probes marked in each column. *Cyp1B1* expression was detected in the anterior and posterior cristae (between arrowheads in **A**, **B**, **G**, **H**, **K**, **L**). The utricular and sacular maculae, as well as the basilar papilla, were *Cyp1B1* positive (mu and ms in **C**, **C'**; bp in **E**), the macula neglecta being *Cyp1B1* negative (mn in **C**). At stage HH24, the lateral crista was *Cyp1B1* negative (lc in c, d). ***Cyp1B1* expression patterns at stage HH25.** (**G-L**) Horizontal sections. Innervation was identified by 3A10 immunoreaction. At stage HH25, the lateral crista was *Cyp1B1* positive (lc in **I**, **J**). The white and purple asterisks in **A**, **C**, **E**, **G**, **I**, and **K** indicate the areas of the mesenchyme expressing or not, respectively, the *Cyp1B1* gene. In the AVG, the *Cyp1B1* expression was evident (short arrows in **G**, **H**). **M**, **N:** 3D diagrams of *Cyp1B1* and *Fgf10* expression patterns in both anterior (**M**) and posterior view (**N**) of the stage HH24/25 inner ear. Dotted areas show the *Fgf10*-positive sensory domain. For the abbreviations, see the list. Orientation: A, anterior; D, dorsal; M, medial; P, posterior.

**Fig. 3. *Cyp1B1* expression patterns at stage HH27. A-H:** Horizontal sections through the inner ear anlage, treated with *Cyp1B1*. *Fgf10* expression was used to identify sensory patches in the developing otic epithelium (**B**, **D**, **F**, **H**). *Cyp1B1* expression was detected in all the cristae (ac, pc, and lc; between arrowheads in **A-D**). The utricular, saccular, and lagenar maculae showed a weaker *Cyp1B1* expression (mu and ms in **C**, **C'**; ml in **G**).

The basilar papilla was also *Cyp1B1* positive (bp; between arrowheads in **E**). In the cochlear duct wall, its rostralmost portion, contiguous to the basilar papilla (bp), was *Cyp1B1* stained (arrows in **E**, **F**). The acoustic-vestibular ganglion was *Cyp1B1* negative (AVG in **C**; see also AG in **E**). The white asterisks in **A**, **C**, **C'**, and **e** indicate the *Cyp1B1* expression in the near mesenchyme, whereas the purple asterisks in **A** and **C** label the mesenchyme without *Cyp1B1* expression. **I**, **J:** 3D diagrams of *Cyp1B1* and *Fgf10* expression patterns in both anterior (**I**) and posterior view (**J**) of the stage HH27 inner ear. Dotted areas show the *Fgf10*-positive sensory domain. For the abbreviations, see the list. Orientation: A, anterior; D, dorsal; M, medial; P, posterior.

**Fig. 4. *Cyp1B1* expression patterns at stage HH34.** Horizontal sections treated with the *Cyp1B1* probes. *Cyp1B1* expression was detected in all the cristae (ac, pc, and lc; between arrowheads in **A**, **B**). The utricular and saccular maculae showed *Cyp1B1* expression (mu and ms in **B**), as well as the macula lagena (ml in **D**), which showed weaker expression. The macula neglecta was *Cyp1B1* negative (mn in **A**). The basilar papilla displayed a decreasing rostral-to-caudal gradient of *Cyp1B1* expression (bp; between arrowheads in **C**). All the non-sensory elements were devoid of *Cyp1B1* transcripts (as examples, see ed and cc in **A**; tv in **C**) except for a small area of the proximal cochlear duct (cd; arrow in **B**). The vestibular and acoustic ganglia were *Cyp1B1* negative (VG in **B'**; AG in **C**). The white asterisks in **A**-**D** indicate the mesenchyme expressing the *Cyp1B1* gene. **E, F:** 3D diagrams of *Cyp1B1* and *Fgf10* expression patterns in both anterior (**E**) and posterior view (**F**) of the stage HH34 inner ear. Dotted areas show the *Fgf10*-positive sensory domain. For the abbreviations, see the list. Orientation: A, anterior; D, dorsal; M, medial; P, posterior; R rostral.



## References

Alsina B, Giraldez F, Pujades C. 2009. Patterning and cell fate in ear development. Int J Dev Biol 53:1503–1513

Alsina B, Whitfield TT. 2017. Sculpting the labyrinth: Morphogenesis of the developing inner ear. Semin Cell Dev Biol 65:47–59

Badeeb OM, Micheal S, Koenekoop RK, den Hollader AI, Hedrawi MT. 2014. CYP1B1 mutations in patients with primary congenital glaucoma from Saudi Arabia. BMC Med Genet 15:109

Baldwin WS, Marko PB, Nelson DR. 2009. The cytochrome P450 (CYP) gene superfamily in Daphnia pulex. BMC Genomics 10:169

Balmer JE, Blomhoff R. 2002. Gene expression regulation by retinoic acid. J Lipid Res 43:1773–1808

Basch ML, Brown RM, Jen HI, Groves AK. 2016. Where hearing starts: the development of the mammalian cochlea. J Anat 228:233–254

Bejjani BA, Xu L, Armstrong D, Lupski JR, Reneker LW. 2002. Expression patterns of cytochrome P4501B1 (Cyp1b1) in FVB/N mouse eyes. Exp Eye Res 75:249–257

Benbrook DM, Chambon P, Rochette-Egly C, Asson-Batres MA. 2014. History of retinoic acid receptors. Subcell Biochem 70:1–20

Bhattacharyya KK, Brake PB, Eltom SE, Otto SA, Jefcoate CR. 1995. Identification of a rat adrenal cytochrome P450 active in polycyclic hydrocarbon metabolism as rat CYP1B1. Demonstration of a unique tissue-specific pattern of hormonal and aryl hydrocarbon receptor-linked regulation. J Biol Chem 270:11595–11602

Blentic A, Gale E, Maden M. 2003. Retinoic acid signalling centres in the avian embryo identified by sites of expression of synthesising and catabolising enzymes. Dev Dyn 227:114–127

Blomhoff R, Blomhoff HK. 2006. Overview of retinoid metabolism and function. J Neurobiol 66:606–630

Bok J, Chang W, Wu DK. (2007). Patterning and morphogenesis of the vertebrate inner ear. Int J Dev Biol 51:521–533

Bok J, Raft S, Kong KA, Koo SK, Drager UC, Wu DK. 2011. Transient retinoic acid signaling confers anterior-posterior polarity to the inner ear. Proc Natl Acad Sci USA 108:161–166

Braunstein EM, Monks DC, Aggarwal VS, Arnold JS, Morrow BE. 2009. Tbx1 and Brn4 regulate retinoic acid metabolic genes during cochlear morphogenesis. BMC Dev Biol 9:31

Buters JT, Sakai S, Richter T, Pineau T, Alexander DL, Savas U, Doehmer J, Ward JM, Jefcoate CR, Gonzalez FJ. 1999. Cytochrome P450 CYP1B1 determines susceptibility to 7, 12-dimethylbenz[a]anthracene-induced lymphomas. Proc Natl Acad Sci USA 96:1977–1982

Cadot S, Frenz D, Maconochie M. 2012. A novel method for retinoic acid administration reveals differential and dose-dependent downregulation of Fgf3 in the developing inner ear and anterior CNS. Dev Dyn 241:741–758

Chambers D, Wilson L, Maden M, Lumsden A. 2007. RALDH-independent generation of retinoic acid during vertebrate embryogenesis by CYP1B1. Development 134:1369–1383

Chatterjee S, Kraus P, Lufkin T. 2010. A symphony of inner ear developmental control genes. BMC Genet 11:68

Chavarria-Soley G, Sticht H, Aklillu E, Ingelman-Sundberg M, Pasutto F, Reis A, Rautenstrauss B. 2008. Mutations in CYP1B1 cause primary congenital glaucoma by reduction of either activity or abundance of the enzyme. Hum Mutat 29:1147–1153

Chen H, Howald WN, Juchau MR. 2000. Biosynthesis of all-trans-retinoic acid from all-trans-retinol: catalysis of all-trans-retinol oxidation by human P-450 cytochromes. Drug Metab Dispos 28:315–322

Chen J, Streit A. 2013. Induction of the inner ear: stepwise specification of otic fate from multipotent progenitors. Hear Res 297:3–12

Choo D, Sanne JL, Wu DK. 1998. The differential sensitivities of inner ear structures to retinoic acid during development. Dev Biol 204:136–150

Choudhary D, Jansson I, Schenkman JB, Sarfarazi M, Stoilov I. 2003. Comparative expression profiling of 40 mouse cytochrome P450 genes in embryonic and adult tissues. Arch Biochem Biophys 414:91–100

Choudhary D, Jansson I, Stoilov I, Sarfarazi M, Schenkman JB. 2004. Metabolism of retinoids and arachidonic acid by human and mouse cytochrome P450 1b1. Drug Metab Dispos 32:840–847

Choudhary D, Jansson I, Stoilov I, Sarfarazi M, Schenkman JB. 2005. Expression patterns of mouse and human CYP orthologs (families 1-4) during development and in different adult tissues. Arch Biochem Biophys 436:50–61

Christou M, Savas U, Schroeder S, Shen X, Thompson T, Gould MN, Jefcoate CR. 1995. Cytochromes CYP1A1 and CYP1B1 in the rat mammary gland: cell-specific expression and regulation by polycyclic aromatic hydrocarbons and hormones. Mol Cell Endocrinol 115:41–50

Dejong CA, Wilson JY. 2014. The Cytochrome P450 superfamily complement (CYPome) in the annelid Capitella teleta. PLoS ONE 9:e107728

Díaz-Hernández ME, Bustamante M, Galván-Hernández CI, Chimal-Monroy J. 2013) Irx1 and Irx2 are coordinately expressed and regulated by retinoic acid, TGFβ and FGF signaling during chick hindlimb development. PLoS ONE 8:e58549

Diez del Corral R, Olivera-Martinez I, Goriely A, Gale E, Maden M, Storey K. 2003. Opposing FGF and retinoid pathways control ventral neural pattern, neuronal differentiation, and segmentation during body axis extension. Neuron 40:65–79

Doshi M, Marcus C, Bejjani BA, Edward DP. 2006. Immunolocalization of CYP1B1 in normal, human, fetal and adult eyes. Exp Eye Res 82:24–32

Dubey A, Rose RE, Jones DR, Saint-Jeannet JP. 2018. Generating retinoic acid gradients by local degradation during craniofacial development: One cell's cue is another cell's poison. Genesis 56

Duester G, Mic FA, Molotkov A. 2003. Cytosolic retinoid dehydrogenases govern ubiquitous metabolism of retinol to retinaldehyde followed by tissue-specific metabolism to retinoic acid. Chem Biol Interact 143–144:201–210

Durston AJ. 2015. Time, space and the vertebrate body axis. Semin Cell Dev Biol 42:66–77

Ebeid M, Huh SH. 2017. FGF signaling: diverse roles during cochlear development. BMB Rep 50:487–495

El-kady MAH, Mitsuo R, Kaminishi Y, Itakura T. 2004a. cDNA cloning, sequence analysis and expression of 3-methylcholanthrene-inducible cytochrome P450 1B1 in carp (Cyprinus carpio). Environ Sci 11:231–240

El-kady MAH, Mitsuo R, Kaminishi Y, Itakura T. 2004b. Isolation of cDNA of novel cytochrome P450 1B gene, CYP1B2, from Carp (Cyprinus carpio) and its induced expression in gills. Environ Sci 11:345–354

Fekete DM, Wu DK. 2002. Revisiting cell fate specification in the inner ear. Curr Opin Neurobiol 12:35–42

Ferran JL, Ayad A, Merchan P, Morales-Delgado N, Sanchez-Arrones L, Alonso A, Sandoval JE, Bardet SM, Corral-San-Miguel R, Sanchez-Guardado LO, Hidalgo-Sanchez M, Martinez-de-laTorre M, Puelles L. 2015. Exploring Brain Genoarchitecture by Single and Double Chromogenic In Situ Hybridization (ISH) and Immunohistochemistry (IHC) on Cryostat, Paraffin, or Floating Sections. In: Hauptmann G (ed) In Situ Hybridization Methods. Springer New York, New York, NY, pp 83–107

Frank D, Sela-Donenfeld D. 2019. Hindbrain induction and patterning during early vertebrate development. Cell Mol Life Sci 76:941–960

Frenz DA, Liu W, Cvekl A, Xie Q, Wassef L, Quadro L, Niederreither K, Maconochie M, Shanske A. 2010. Retinoid signaling in inner ear development: A "Goldilocks" phenomenon. Am J Med Genet A 152A:2947–2961

Fritzsch B, Elliott KL. 2017. Gene, cell, and organ multiplication drives inner ear evolution. Dev Biol 431:3–15

Glover JC, Renaud JS, Rijli FM. 2006. Retinoic acid and hindbrain patterning. J Neurobiol 66:705–725

Godard CA, Leaver MJ, Said MR, Dickerson RL, George S, Stegeman JJ. 2000. Identification of cytochrome P450 1B-like sequences in two teleost fish species (scup, Stenotomus chrysops and plaice, Pleuronectes platessa) and in a cetacean (striped dolphin, Stenella coeruleoalba). Mar Environ Res 50:7–10

Godard CA, Goldstone JV, Said MR, Dickerson RL, Woodin BR, Stegeman JJ. 2005. The new vertebrate CYP1C family: cloning of new subfamily members and phylogenetic analysis. Biochem Biophys Res Commun 331:1016–1024

Gomez-Skarmeta JL, Glavic A, de la Calle-Mustienes E, Modolell J, Mayor R. 1998. Xiro, a Xenopus homolog of the Drosophila Iroquois complex genes, controls development at the neural plate. EMBO J 17:181–190

Groves AK, Fekete DM. 2012. Shaping sound in space: the regulation of inner ear patterning. Development 139:245–257

Gudas LJ, Wagner JA. 2011. Retinoids regulate stem cell differentiation. J Cell Physiol 226:322–330

Hamburger V, Hamilton HL. 1951. A series of normal stages in the development of the chick embryo. J Morphol 88:49–92

Hans S, Westerfield M. 2007. Changes in retinoic acid signaling alter otic patterning. Development 134:2449–2458

Itakura T, El-Kady M, Mitsuo R, Kaminishi Y. 2005. Complementary DNA cloning and constitutive expression of cytochrome P450 1C1 in the gills of carp (Cyprinus carpio). Environ Sci 12:111–120

Jonsson ME, Orrego R, Woodin BR, Goldstone JV, Stegeman JJ. 2007. Basal and 3,3',4,4',5-pentachlorobiphenyl-induced expression of cytochrome P450 1A, 1B and 1C genes in zebrafish. Toxicol Appl Pharmacol 221:29–41

Ladher RK, O'Neill P, Begbie J. 2010. From shared lineage to distinct functions: the development of the inner ear and epibranchial placodes. Development 137:1777–1785

Lassiter RNT, Stark MR, Zhao T, Zhou CJ. 2014. Signaling mechanisms controlling cranial placode neurogenesis and delamination. Dev Biol 389:39–49

Liu W, Levi G, Shanske A, Frenz DA. 2008. Retinoic acid-induced inner ear teratogenesis caused by defective Fgf3/Fgf10-dependent Dlx5 signaling. Birth Defects Res B Dev Reprod Toxicol 83:134–144

Lupo G, Liu Y, Qiu R, Chandraratna RA, Barsacchi G, He RQ, Harris WA. 2005. Dorsoventral patterning of the Xenopus eye: a collaboration of Retinoid, Hedgehog and FGF receptor signaling. Development 132:1737–1748

Maden M. 2006. Retinoids and spinal cord development. J Neurobiol 66:726–738

Maier EC, Whitfield TT. 2014. RA and FGF signalling are required in the zebrafish otic vesicle to pattern and maintain ventral otic identities. PLoS Genet 10:e1004858

Mark M, Ghyselinck NB, Chambon P. 2006. Function of retinoid nuclear receptors: lessons from genetic and pharmacological dissections of the retinoic acid signaling pathway during mouse embryogenesis. Annu Rev Pharmacol Toxicol 46:451–480

McCaffery P, Dräger UC. 2000. Regulation of retinoic acid signaling in the embryonic nervous system: a master differentiation factor. Cytokine Growth Factor Rev 11:233–249

Meinhardt H. 2008. Models of biological pattern formation: from elementary steps to the organization of embryonic axes. Curr Top Dev Biol 81:1–63

Mic FA, Molotkov A, Fan X, Cuenca AE, Duester G. 2000. RALDH3, a retinaldehyde dehydrogenase that generates retinoic acid, is expressed in the ventral retina, otic vesicle and olfactory pit during mouse development. Mech Dev 97:227–230

Monks DC, Morrow BE. 2012. Identification of putative retinoic acid target genes downstream of mesenchymal Tbx1 during inner ear development. Dev Dyn 241:563–573

Munnamalai V, Fekete DM. 2013. Wnt signaling during cochlear development. Semin Cell Dev Biol 24:480–489

Murray GI, Melvin WT, Greenlee WF, Burke MD. 2001. Regulation, function, and tissue-specific expression of cytochrome P450 CYP1B1. Annu Rev Pharmacol Toxicol 41:297–316

Murray GI, Taylor MC, McFadyen MC, McKay JA, Greenlee WF, Burke MD, Melvin WT. 1997. Tumor-specific expression of cytochrome P450 CYP1B1. Cancer Res 57:3026–3031

Nakajima Y. 2015. Signaling regulating inner ear development: cell fate determination, patterning, morphogenesis, and defects. Congenit Anom (Kyoto) 55:17–25

Nelson DR. 2011. Progress in tracing the evolutionary paths of cytochrome P450. Biochim Biophys Acta 1814:14–18

Nelson DR. 2018. Cytochrome P450 diversity in the tree of life. Biochim Biophys Acta Proteins Proteom 1866:141–154

Niederreither K, Dollé P. 2006. Molecular mediators of retinoic acid signaling during development. In: Advances in Developmental Biology. Elsevier, pp 105–143

Niederreither K, Fraulob V, Garnier JM, Chambon P, Dollé P. 2002. Differential expression of retinoic acid-synthesizing (RALDH) enzymes during fetal development and organ differentiation in the mouse. Mech Dev 110:165–171

Niederreither K, Vermot J, Schuhbaur B, Chambon P, Dollé P. 2000. Retinoic acid synthesis and hindbrain patterning in the mouse embryo. Development 127:75–85

Novitch BG, Wichterle H, Jessell TM, Sockanathan S. 2003. A requirement for retinoic acid-mediated transcriptional activation in ventral neural patterning and motor neuron specification. Neuron 40:81–95

Ohta S, Schoenwolf GC. 2018. Hearing crosstalk: the molecular conversation orchestrating inner ear dorsoventral patterning. Wiley Interdiscip Rev Dev Biol 7

Ohyama T, Groves AK, Martin K. 2007. The first steps towards hearing: mechanisms of otic placode induction. Int J Dev Biol 51:463–472

Olaya-Sánchez D, Sánchez-Guardado LÓ, Ohta S, Chapman SC, Schoenwolf GC, Puelles L, Hidalgo-Sánchez M. 2017. Fgf3 and Fgf16 expression patterns define spatial and temporal domains in the developing chick inner ear. Brain Struct Funct 222:131–149

Otto S, Bhattacharyya KK, Jefcoate CR. 1992. Polycyclic aromatic hydrocarbon metabolism in rat adrenal, ovary, and testis microsomes is catalyzed by the same novel cytochrome P450 (P450RAP). Endocrinology 131:3067–3076

Otto S, Marcus C, Pidgeon C, Jefcoate C. 1991. A novel adrenocorticotropin-inducible cytochrome P450 from rat adrenal microsomes catalyzes polycyclic aromatic hydrocarbon metabolism. Endocrinology 129:970–982

Palenski TL, Sorenson CM, Jefcoate CR, Sheibani N. 2013. Lack of Cyp1b1 promotes the proliferative and migratory phenotype of perivascular supporting cells. Lab Invest 93:646–662

Pennimpede T, Cameron DA, MacLean GA, Li H, Abu-Abed S, Petkovich M. 2010. The role of CYP26 enzymes in defining appropriate retinoic acid exposure during embryogenesis. Birth Defects Res Part A Clin Mol Teratol 88:883–894

Piersma AH, Hessel EV, Staal YC. 2017. Retinoic acid in developmental toxicology: Teratogen, morphogen and biomarker. Reprod Toxicol 72:53–61

Pottenger LH, Christou M, Jefcoate CR. 1991. Purification and immunological characterization of a novel cytochrome P450 from C3H/10T1/2 cells. Arch Biochem Biophys 286:488–497

Raft S, Groves AK. 2015a. Segregating neural and mechanosensory fates in the developing ear: patterning, signaling, and transcriptional control. Cell Tissue Res 359:315–332

Raft S, Groves AK. 2015b. Segregating neural and mechanosensory fates in the developing ear: patterning, signaling, and transcriptional control. Cell Tissue Res 359:315–332

Romand R, Albuisson E, Niederreither K, Fraulob V, Chambon P, Dolle P. 2001. Specific expression of the retinoic acid-synthesizing enzyme RALDH2 during mouse inner ear development. Mech Dev 106:185–189

Romand R, Dollé P, Hashino E. 2006. Retinoid signaling in inner ear development. J Neurobiol 66:687–704

Romand R, Niederreither K, Abu-Abed S, Petkovich M, Fraulob V, Hashino E, Dolle P. (2004). Complementary expression patterns of retinoid acid-synthesizing and -metabolizing enzymes in pre-natal mouse inner ear structures. Gene Expression Patterns 4:123–133

Roselló-Díez A, Arques CG, Delgado I, Giovinazzo G, Torres M. 2014. Diffusible signals and epigenetic timing cooperate in late proximo-distal limb patterning. Development 141:1534–1543

Ross SA, McCaffery PJ, Drager UC, De Luca LM. 2000. Retinoids in embryonal development. Physiol Rev 80:1021–1054

Sanchez-Calderon H, Milo M, Leon Y, Varela-Nieto I. 2007. A network of growth and transcription factors controls neuronal differentation and survival in the developing ear. Int J Dev Biol 51:557–570

Sanchez-Guardado LO, Ferran JL, Mijares J, Puelles L, Rodriguez-Gallardo L, Hidalgo-Sanchez M. 2009. Raldh3 gene expression pattern in the developing chicken inner ear. J Comp Neurol 514:49–65

Sanchez-Guardado LO, Ferran JL, Rodriguez-Gallardo L, Puelles L, Hidalgo-Sanchez M. 2011. Meis gene expression patterns in the developing chicken inner ear. J Comp Neurol 519:125–147

Sánchez-Guardado LÓ, Puelles L, Hidalgo-Sánchez M. 2014. Fate map of the chicken otic placode. Development 141:2302–2312

Sánchez-Guardado LÓ, Puelles L, Hidalgo-Sánchez M. 2013. Fgf10 expression patterns in the developing chick inner ear. J Comp Neurol 521:1136–1164

Savas U, Bhattacharyya KK, Christou M, Alexander DL, Jefcoate CR. 1994. Mouse cytochrome P-450EF, representative of a new 1B subfamily of cytochrome P-450s. Cloning, sequence determination, and tissue expression. J Biol Chem 269:14905–14911

Savory JG, Edey C, Hess B, Mears AJ, Lohnes D. 2014. Identification of novel retinoic acid target genes. Dev Biol 395:199–208

Schilling TF, Nie Q, Lander AD. 2012. Dynamics and precision in retinoic acid morphogen gradients. Curr Opin Genet Dev 22:562–569

Schimmang T. 2007. Expression and functions of FGF ligands during early otic development. Int J Dev Biol 51:473–481

Schneider-Maunoury S, Pujades C. 2007. Hindbrain signals in otic regionalization: walk on the wild side. Int J Dev Biol 51:495–506

Shimada T, Hayes CL, Yamazaki H, Amin S, Hecht SS, Guengerich FP, Sutter TR. 1996. Activation of chemically diverse procarcinogens by human cytochrome P-450 1B1. Cancer Res 56:2979–2984

Sissung TM, Price DK, Sparreboom A, Figg WD. 2006. Pharmacogenetics and regulation of human cytochrome P450 1B1: implications in hormone-mediated tumor metabolism and a novel target for therapeutic intervention. Mol Cancer Res 4:135–150

Stefanovic S, Zaffran S. 2017. Mechanisms of retinoic acid signaling during cardiogenesis. Mech Dev 143:9–19

Stoilov I, Rezaie T, Jansson I, Schenkman JB, Sarfarazi M. 2004. Expression of cytochrome P4501b1 (Cyp1b1) during early murine development. Mol Vis 10:629–636

Su YX, Hou CC, Yang WX.(2015. Control of hair cell development by molecular pathways involving Atoh1, Hes1 and Hes5. Gene 558:6–24

Sutter TR, Tang, YM, Hayes CL, Wo YY, Jabs EW, Li X, Yin H, Cody CW, Greenlee WF. 1994. Complete cDNA sequence of a human dioxin-inducible mRNA identifies a new gene subfamily of cytochrome P450 that maps to chromosome 2. J Biol Chem 269:13092–13099

Tang YM, Wo YY, Stewart J, Hawkins AL, Griffin CA, Sutter TR, Greenlee WF. 1996. Isolation and characterization of the human cytochrome P450 CYP1B1 gene. J Biol Chem 271:28324–28330

Thatcher JE, Isoherranen N. 2009. The role of CYP26 enzymes in retinoic acid clearance. Expert Opin Drug Metab Toxicol 5:875–886

Thiede BR, Mann ZF, Chang W, Ku YC, Son YK, Lovett M, Kelley MW, Corwin JT. 2014. Retinoic acid signalling regulates the development of tonotopically patterned hair cells in the chicken cochlea. Nat Commun 5:3840

Thompson DL, Gerlach-Bank LM, Barald KF, Koenig RJ. 2003. Retinoic Acid Repression of Bone Morphogenetic Protein 4 in Inner Ear Development. Molecular and Cellular Biology 23:2277–2286

Tonk ECM, Pennings JLA, Piersma AH. 2015. An adverse outcome pathway framework for neural tube and axial defects mediated by modulation of retinoic acid homeostasis. Reprod Toxicol 55:104–113

Tuazon FB, Mullins MC. 2015. Temporally coordinated signals progressively pattern the anteroposterior and dorsoventral body axes. Semin Cell Dev Biol 42:118–133

Varela-Nieto I, Palmero I, Magariños M. 2019. Complementary and distinct roles of autophagy, apoptosis and senescence during early inner ear development. Hear Res 376:86–96

Vasiliou V, Gonzalez FJ. 2008. Role of CYP1B1 in glaucoma. Annu Rev Pharmacol Toxicol 48:333–358

White RJ, Schilling TF. 2008. How degrading: Cyp26s in hindbrain development. Dev Dyn 237:2775–2790

Whitfield TT. 2015. Development of the inner ear. Curr Opin Genet Dev 32:112–118

Whitfield TT, Hammond KL. 2007. Axial patterning in the developing vertebrate inner ear. Int J Dev Biol 51:507–520

Williams AL, Eason J, Chawla B, Bohnsack BL. 2017. Cyp1b1 Regulates Ocular Fissure Closure Through a Retinoic Acid-Independent Pathway. Invest Ophthalmol Vis Sci 58:1084–1097

Wilson L, Maden M. 2005. The mechanisms of dorsoventral patterning in the vertebrate neural tube. Dev Biol 282:1–13

Wu DK, Kelley MW. 2012. Molecular mechanisms of inner ear development. Cold Spring Harb Perspect Biol 4:a008409

Xavier-Neto J, Sousa Costa ÂM, Figueira AC, Caiaffa CD, Amaral FN, Peres LM, da Silva BS, Santos LN, Moise AR, Castillo HA. 2015. Signaling through retinoic acid receptors in cardiac development: Doing the right things at the right times. Biochim Biophys Acta 1849:94–111

Xu M, Miller MS. 2004. Determination of murine fetal Cyp1a1 and 1b1 expression by real-time fluorescence reverse transcription-polymerase chain reaction. Toxicol Appl Pharmacol 201:295–302

Yin HC, Tseng HP, Chung HY, Ko CY, Tzou WS, Buhler DR, Hu CH. 2008. Influence of TCDD on zebrafish CYP1B1 transcription during development. Toxicol Sci 103:158–168

Zhang QY, Dunbar D, Kaminsky L. 2000. Human cytochrome P-450 metabolism of retinals to retinoic acids. Drug Metab Dispos 28:292–297

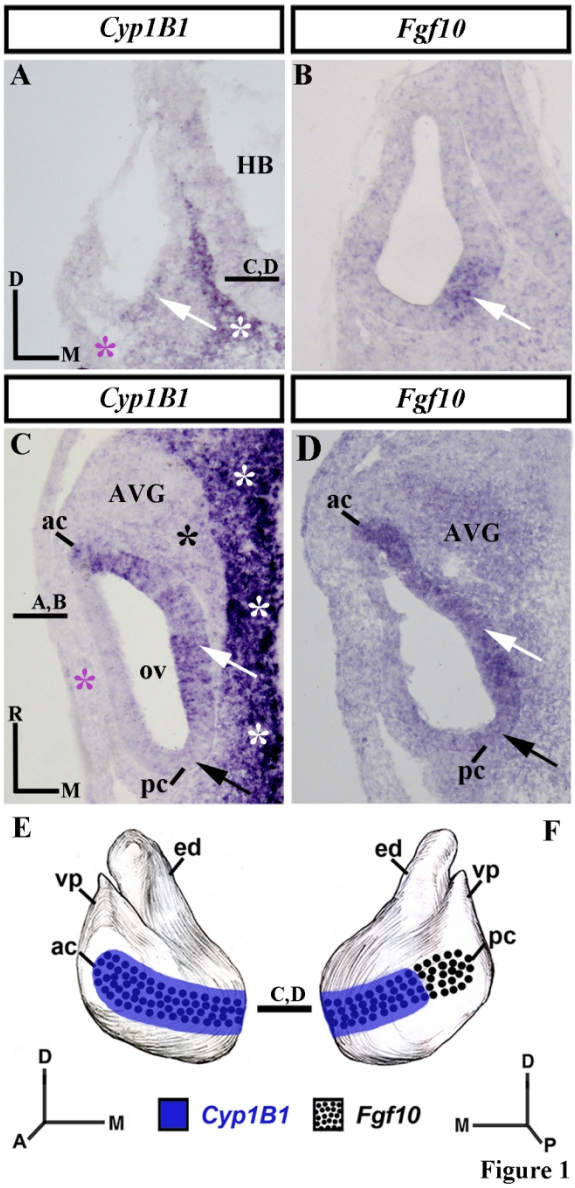


Figure 1

Fig. 1. Cyp1B1 expression pattern at the otic vesicle stage, HH18-20. Transverse (A, B) and horizontal (C, D) sections were treated with the Cyp1B1 and Fgf10 probes. The Cyp1B1 and Fgf10 expressions were observed in the medial wall of the otic vesicle (white arrows in A-D), excluding the presumptive domain of the Fgf10-stained posterior crista (pc; back arrows in C, D). The black asterisk in c designates a weak Cyp1B1 expression in the acoustic-vestibular ganglion. The white and purple asterisks in A and C label the periotic mesenchyme expressing or not the Cyp1B1 gene, respectively. E, D: 3D diagrams of Cyp1B1 expression patterns at the otic vesicle stage, HH18-20, in anterior (E) and posterior (D) views. Dotted areas show the Fgf10-positive sensory domain. For other abbreviations, see the list. Orientation: A, anterior; D, dorsal; M, medial; P, posterior.

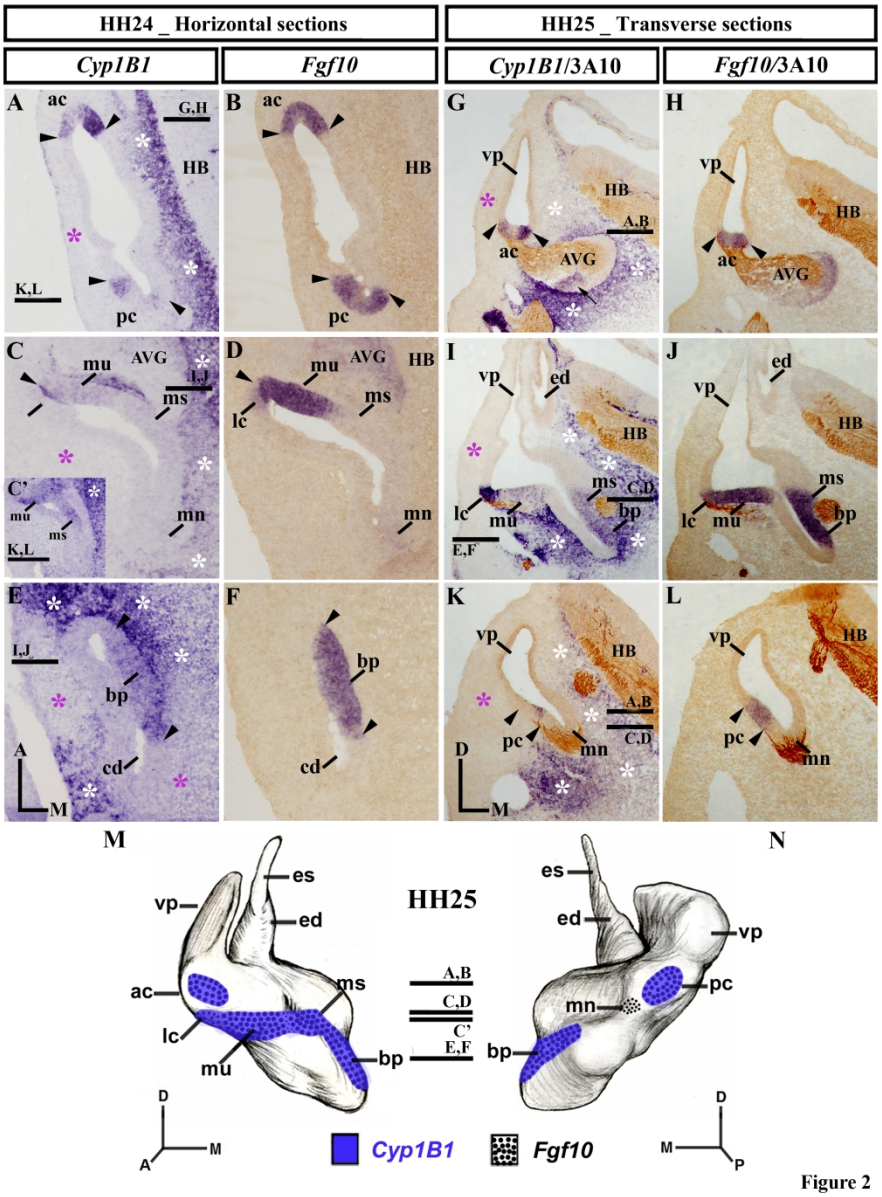


Figure 2

Fig. 2. Cyp1B1 expression patterns at stage HH24. A-F: Horizontal sections treated with the probes marked in each column. Cyp1B1 expression was detected in the anterior and posterior cristae (between arrowheads in A, B, G, H, K, L). The utricular and sacular maculae, as well as the basilar papilla, were Cyp1B1 positive (mu and ms in C, C'; bp in E), the macula neglecta being Cyp1B1 negative (mn in C). At stage HH24, the lateral crista was Cyp1B1 negative (lc in c, d). Cyp1B1 expression patterns at stage HH25. (G-L) Horizontal sections. Innervation was identified by 3A10 immunoreaction. At stage HH25, the lateral crista was Cyp1B1 positive (lc in I, J). The white and purple asterisks in A, C, E, G, I, and K indicate the areas of the mesenchyme expressing or not, respectively, the Cyp1B1 gene. In the AVG, the Cyp1B1 expression was evident (short arrows in G, H). M, N: 3D diagrams of Cyp1B1 and Fgf10 expression patterns in both anterior (M) and posterior view (N) of the stage HH24/25 inner ear. Dotted areas show the Fgf10-positive sensory domain. For the abbreviations, see the list. Orientation: A, anterior; D, dorsal; M, medial; P, posterior.

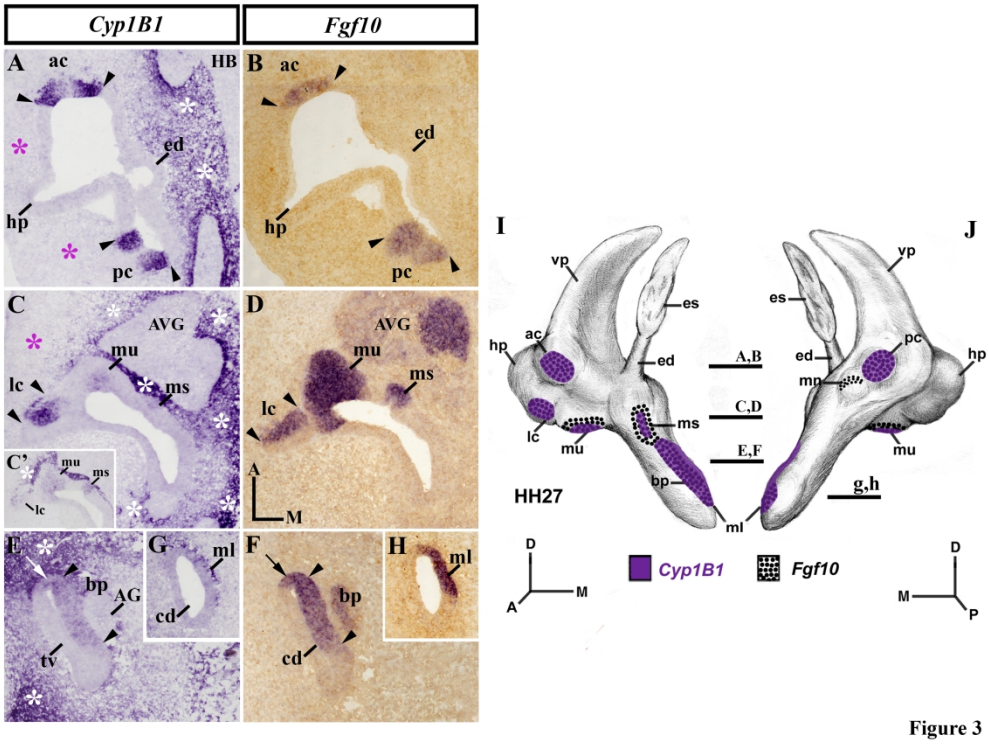


Figure 3

Fig. 3. Cyp1B1 expression patterns at stage HH27. A-H: Horizontal sections through the inner ear anlage, treated with Cyp1B1. Fgf10 expression was used to identify sensory patches in the developing otic epithelium (B, D, F, H). Cyp1B1 expression was detected in all the cristae (ac, pc, and lc; between arrowheads in A-D). The utricular, saccular, and lagenar maculae showed a weaker Cyp1B1 expression (mu and ms in C, C'; ml in G). The basilar papilla was also Cyp1B1 positive (bp; between arrowheads in E). In the cochlear duct wall, its rostralmost portion, contiguous to the basilar papilla (bp), was Cyp1B1 stained (arrows in E, F). The acoustic-vestibular ganglion was Cyp1B1 negative (AVG in C; see also AG in E). The white asterisks in A, C, C', and e indicate the Cyp1B1 expression in the near mesenchyme, whereas the purple asterisks in A and C label the mesenchyme without Cyp1B1 expression. I, J: 3D diagrams of Cyp1B1 and Fgf10 expression patterns in both anterior (I) and posterior view (J) of the stage HH27 inner ear. Dotted areas show the Fgf10-positive sensory domain. For the abbreviations, see the list. Orientation: A, anterior; D, dorsal; M, medial; P, posterior.

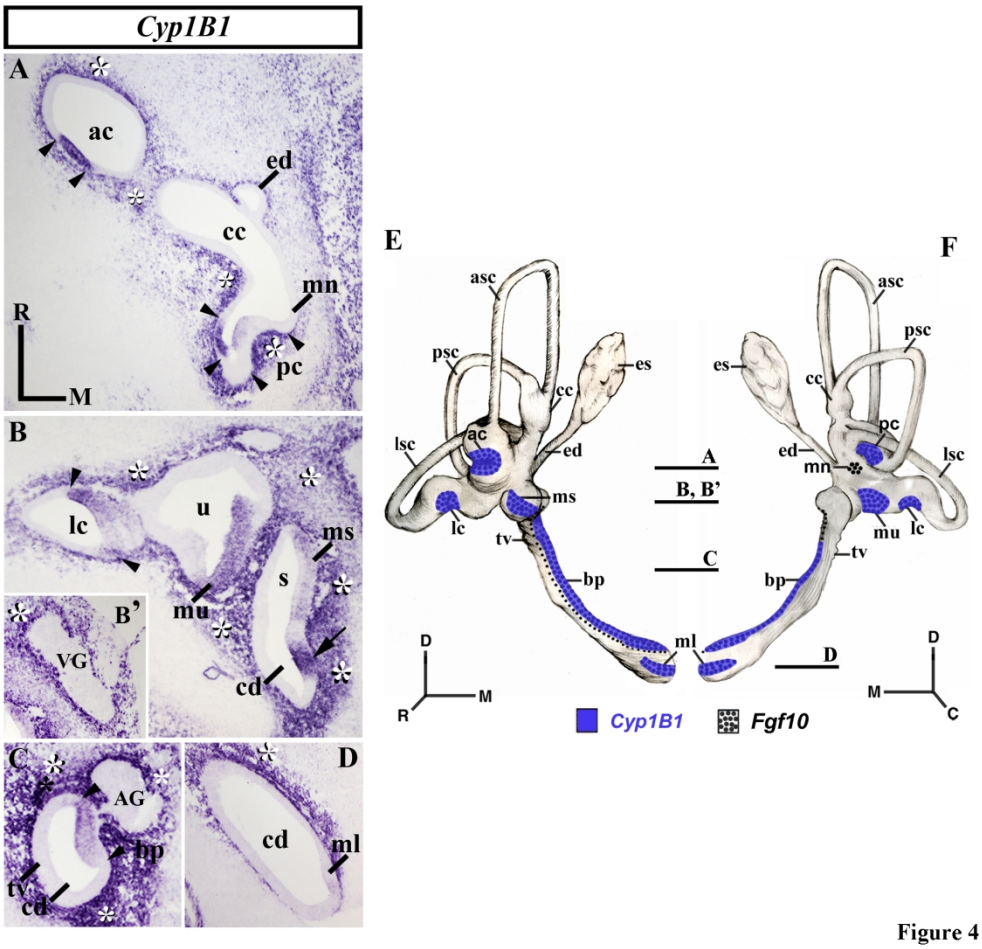


Figure 4

Fig. 4. Cyp1B1 expression patterns at stage HH34. Horizontal sections treated with the Cyp1B1 probes. Cyp1B1 expression was detected in all the cristae (ac, pc, and lc; between arrowheads in A, B). The utricular and saccular maculae showed Cyp1B1 expression (mu and ms in B), as well as the macula lagena (ml in D), which showed weaker expression. The macula neglecta was Cyp1B1 negative (mn in A). The basilar papilla displayed a decreasing rostral-to-caudal gradient of Cyp1B1 expression (bp; between arrowheads in C). All the non-sensory elements were devoid of Cyp1B1 transcripts (as examples, see ed and cc in A; tv in C) except for a small area of the proximal cochlear duct (cd; arrow in B). The vestibular and acoustic ganglia were Cyp1B1 negative (VG in B'; AG in C). The white asterisks in A-D indicate the mesenchyme expressing the Cyp1B1 gene. E, F: 3D diagrams of Cyp1B1 and Fgf10 expression patterns in both anterior (E) and posterior view (F) of the stage HH34 inner ear. Dotted areas show the Fgf10-positive sensory domain. For the abbreviations, see the list. Orientation: A, anterior; D, dorsal; M, medial; P, posterior; R rostral.